*Proc. Natl. Acad. Sci. USA*
Vol. 88, pp. 7451–7455, August 1991
Medical Sciences

# Surfactant protein B: Lipid interactions of synthetic peptides representing the amino-terminal amphipathic domain

(protein secondary structure/amino acid substitutions/lipid–peptide interaction/structure–function relationships/oxygen delivery)

ROBERTA BRUNI*, H. WILLIAM TAEUSCH, AND ALAN J. WARING

Department of Pediatrics, King/Drew Medical Center, University of California, Los Angeles, School of Medicine, Los Angeles, CA 90059

*Communicated by John A. Clements, March 8, 1991*

**ABSTRACT** **The mechanisms by which pulmonary surfactant protein B (SP-B) affects the surface activity of surfactant lipids are unclear. We have studied the peptide/lipid interactions of the amino-terminal amphipathic domain of SP-B by comparing the secondary conformations and surface activities of a family of synthetic peptides based on the native human SP-B sequence, modified by site-specific amino acid substitutions. Circular dichroism measurements show an α-helical structure correlating with the ability of the peptides to interact with lipids and with the surface activity of peptide/lipid dispersions. Amino acid substitutions altering either the charge or the hydrophobicity of the residues lowered the helical content and reduced the association of the amino-terminal segment with lipid dispersions. Surface activity of peptide/lipid mixtures was maximally altered by reversal of charge in synthetic peptides. These observations indicate that electrostatic interactions and hydrophobicity are important factors in determining optimal structure and function of surfactant peptides in lipid dispersions.**

Surfactant protein B (SP-B, $M_r$ 9000; refs. 1 and 2) is encoded on chromosome 2 and synthesized by type 2 pneumocytes (3–6). The primary translation product for SP-B is a 381-residue glycosylated preprotein ($M_r$ 42,000) (7). Amino- and carboxyl-terminal proteolytic cleavage produces a 79-residue peptide, with amino terminus located at residue 201 of the preprotein. Mature SP-B lacks glycosylation sites, is highly hydrophobic, and has a basic pI. In contrast to surfactant protein C (SP-C), SP-B has no covalently linked lipids, although it coisolates with SP-C and surfactant lipids (8). Four of 10 positively charged residues (two arginines, two lysines) appear at the amino terminus. Negatively and positively charged residues are found at the carboxyl terminus (one aspartate, one glutamate, four arginines). Intra- and intermolecular sulfhydryl bonds are important structural features of the mature protein, which contains seven cysteines and is oligomeric under oxidizing conditions (9, 10).

Together with surfactant protein A (SP-A) and SP-C, SP-B interacts with lipids to form mammalian pulmonary surfactant. SP-B is present in lamellar bodies in type II pneumocytes and appears in bronchoalveolar lavage. SP-B from bovine and porcine sources contributes to the function of surfactant preparations used in replacement therapies (11–15). Synthetic SP-B (16) and synthetic peptides from predicted amphipathic sequences of human SP-B (17) emulate native SP-B in surfactant lipid dispersions (13, 16–19).

Quantitative measurements of the amphipathicity of the human amino acid sequence of SP-B using the Eisenberg hydrophobic algorithm (20) predict that the amino-terminal sequence has a high α hydrophobic moment (9, 21). Therefore, we investigated the amino-terminal sequence of SP-B to identify secondary structures and specific conformations associated with surface activity in peptide/lipid dispersions. Based on the native amino-terminal human sequence of SP-B, a 25-amino acid peptide was synthesized, B(1–25) (Table 1). This sequence was modified by specific amino acid substitutions to obtain five additional peptides. These synthetic B(1–25) analogs were compared to investigate the role of individual residues in protein structure and function. We hypothesized that charge, hydrophobicity, size, and potential for oligomerization would impose constraints on the three-dimensional peptide conformation in the different solvating environments used in the study, thereby affecting peptide interaction with surfactant lipids (22).

## MATERIALS AND METHODS

**Rationale for Amino Acid Substitutions.** Synthetic analog peptides of B(1–25) are defined in Table 1. Cysteines 8 and 11 were replaced with alanine residues, to prevent disulfide-dependent oligomerization (A/C). Seven hydrophobic leucine and isoleucine residues were substituted by alanine throughout B(1–25), thereby decreasing the hydrophobicity of the sequence (A/L-I). Specific effects of polar residues were tested by three different substitutions. Arginines in positions 12 and 17 were replaced with lysines, retaining the charge but substituting the guanidinium ring with an aliphatic chain, to reduce the steric hindrance of the residue (K/R). Amphipathicity of the sequence was altered by substituting polar, charged lysines (positions 16 and 24) and arginines (positions 12 and 17) with polar, uncharged serine (S/K-R). The net positive charge of the sequence was reversed by introducing glutamate in positions 12, 16, 17, and 24 (E/K-R).

Secondary structure was predicted by the Chou–Fasman algorithm (23), the Schiffer–Edmundson α-helical wheel (24), and the Eisenberg hydrophobic moment plot (20).

**Peptide Synthesis and Purification.** B(1–25) analogs were synthesized using the solid-phase method of Merrifield, employing a *tert*-butyloxycarbonyl strategy (UCLA Peptide Synthesis Facility) as described (17, 25).

Peptides were purified by reverse-phase HPLC using a water/acetonitrile/0.1% trifluoroacetic acid mixture on a Vydac $C_4$ preparative column. Purified fractions were dried by vacuum centrifugation and the molecular weight of each peptide was confirmed by fast atom bombardment mass spectroscopy (City of Hope, Mass Spectroscopic Facility, Duarte, CA).

**Preparation of Lipid/Peptide Dispersions.** Phospholipids were from Avanti Polar Lipids; palmitic acid was from

The publication costs of this article were defrayed in part by page charge payment. This article must therefore be hereby marked "*advertisement*" in accordance with 18 U.S.C. §1734 solely to indicate this fact.

Abbreviations: SP-A, SP-B, and SP-C, surfactant proteins A, B, and C; FTIR, Fourier transform infrared; DPPC, dipalmitoyl phosphatidylcholine; PG, phosphatidyl glycerol; PA, palmitic acid; SA, stearylamine.

*To whom reprint requests should be addressed at: Department of Pediatrics, King/Drew Medical Center, 12021 South Wilmington Avenue, Los Angeles, CA 90059.

Table 1. Human SP-B sequence for synthetic B(1–25) analogs, in one-letter code

| Peptide | Human SP-B sequence |
|---|---|
| B(1–25) | FPIPLPYCWLCRALIKRIQAMIPKG |
| A/C | ————————A——A———————— |
| A/L-I | ——A—A————A———AA——A———A—— |
| K/R | ———————————K————K————— |
| S/K-R | ———————————S——SS———————S— |
| E/K-R | ———————————E——EE———————E— |

The amino-terminal human sequence of SP-B (7), given in three-letter code, is as follows: $NH_2$-Phe-Pro-Ile-Pro-Leu-Pro-Tyr-Cys-Trp-Leu-Cys-Arg-Ala-Leu-Ile-Lys-Arg-Ile-Gln-Ala-Met-Ile-Pro-Lys-Gly-COOH.

Nu-Chek-Prep (Elysian, MN); solvents were HPLC grade or higher. The standard lipid mixture contained dipalmitoyl phosphatidylcholine (DPPC), egg phosphatidyl glycerol (PG), and palmitic acid (PA), 68:22:9 (wt/wt). These lipids have been employed in several reconstitution studies and are referred to as Tanaka lipids (9, 17, 26). Peptide dispersions in organic solvent were mixed with Tanaka lipids in a molar ratio of 0.8% peptide:lipid and dried under nitrogen stream. The film was resuspended in unbuffered saline (154 mM NaCl, pH 5.3) at 45°C for 1 hr under nitrogen, with intermittent Vortex mixing, at 2.4 mg of lipid per ml.

**Determination of the Distribution of Peptides Between Lipid Dispersions and Bulk Solvent.** The apparent partition coefficient $K_{ap}$ for the peptides was estimated from the concentration of peptide in the aqueous, $[P]_A$, and the lipid, $[P]_L$, phases. The dispersions were kept at 37°C for 12 hr and centrifuged at 100,000 × *g* for 60 min. The centrifugation procedure pelleted the peptide/lipid vesicles leaving free peptide in the aqueous supernatant. Peptide concentration in the supernatant was determined by endogenous tryptophan fluorescence. The partition coefficient was calculated as detailed in Table 2. Fluorescence measurements were made with a Perkin–Elmer LS-5B luminescence spectrometer. Excitation was at 280 nm and emission was at 355 nm, slit width of 10-nm excitation and 15-nm emission. $[P]_L$ was estimated by subtraction of $[P]_A$ from the total peptide concentration $[P]_T$. The lipid density was assumed to be 1 g/ml. The apparent partition coefficient $K_{ap}$ was determined by using the equation $[P]_L = K_{ap} \times [P]_A$.

**Secondary Structure Analysis by Circular Dichroism (CD) Spectroscopy and Fourier Transform Infrared (FTIR) Spectroscopy.** CD spectroscopy was performed on Jasco (Easton, MD) J600 or J720 spectropolarimeters. Measurements were carried out at 37°C, using a rectangular cell with a 0.1-mm path length. The secondary structure of the peptides was assessed in several structure-promoting environments: 25% and 50% trifluoroethanol/5 mM phosphate buffer (TFE/PBS) at pH 4.0, 5.3, and 7.0; 20 mM sodium dodecyl sulfate (SDS) micelles in PBS at pH 5.3 and 7.0; and peptide/lipid dispersions in unbuffered saline at pH 5.3. With the peptide/lipid dispersions, the sample cuvette was positioned close to the photomultiplier, using a SCH-1 cell holder to minimize light scattering artifacts. The instrument was calibrated with an aqueous solution of (+)-10-camphorsulfonic acid (1 mg/ml) in a 1-mm path length cell (27). Samples were scanned from 250 nm to 195 nm, scan rate of 10 nm per minute. Four to eight spectra were averaged, baseline corrected, smoothed, and analyzed for relative $\alpha$-helical content by unrestrained least-squares-fit algorithm (28), based on poly-lysine reference spectra (29).

IR spectra were recorded with a Nicolet 205 FTIR spectrophotometer. The peptide/lipid dispersions were dried onto a zinc selenide attenuated total reflectance crystal (SpectraTech, Stamford, CT) to produce multilayers as described by Rafalski *et al.* (30). Spectra were averaged from 128 scans at a gain of 4 and a spectral resolution of 4 $cm^{-1}$.

**Surface Pressure Measurements of Peptide/Lipid Interactions.** The tendency of a peptide to interact with a lipid structure was estimated from changes in surface pressure ($\Delta\pi$) following injection of dilute peptides underneath lipid monolayers spread at various initial surface pressures $\pi_i$ (31–33). Increases in $\pi$ are due to association and insertion of the peptide into the lipid monolayer. The critical pressure of insertion ($\pi_c$) is defined as the theoretical $\pi_i$ of the monolayer at which no further change in $\pi$ occurs when a peptide is injected, as obtained from the equation: $y = Ax + B$ for $y = 0$, where $x$ is $\pi_i$ and $y$ is the $\Delta\pi$ obtained after injection of the peptide. Experimental values for parameters A and B in each plot were obtained by linear regression. Parameter A, the slope of the plot, measures the affinity of the peptide for the lipids. Parameter B represents the equilibrium $\pi$ extrapolated for $\pi_i = 0$, and it is higher than the actual equilibrium $\pi$ of the peptide on a clean saline surface.

Measurements were carried out on a King–Clements device (17). A saline hypophase was stirred at 120 rpm in a round Teflon trough (44.2 $cm^2$) at 37°C. Changes in surface tension vs. time were recorded by an electronic force transducer (Sensotec, Columbus, OH) coupled to a Hewlett–Packard 7044 B *x–y* recorder/amplifier. Lipid aliquots in chloroform, 1 mg/ml, were spread on the hypophase and the surface tension of the resulting monolayer was measured after evaporation of the organic solvent. $\pi_i$ is the difference between the surface tension of the clean saline surface and that of the lipid monolayer.

To investigate peptide specificity for lipids (34), B(1–25) was tested with lipid monolayers of different composition: DPPC alone; DPPC:PG, 3:1; DPPC:PG:PA, 68:22:9; and DPPC:stearylamine (SA):PA, 68:7:9 (wt/wt). Subsequently, human serum albumin (fraction V, globulin free, Sigma), B(1–25), A/C, A/L-I, K/R, S/K-R, and E/K-R were compared using a monolayer of Tanaka lipids.

Ten-microliter samples of peptide dispersions in saline/isopropyl alcohol were injected in the stirred hypophase, and adsorption was allowed to occur over 30 min. Injection of solvent alone did not affect $\pi$. In preliminary experiments, concentrations of B(1–25) between 1 and 4 $\mu$M were all found to exert a $\pi$ of 26 ± 0.5 mN/m when adsorbed to a clean saline surface. Within this concentration range, we selected 2.5 $\mu$M for all subsequent experiments. At this concentration albumin, used as a reference protein (35, 36), appears to aggregate and was therefore compared to B(1–25) only at 1 $\mu$M concentrations.

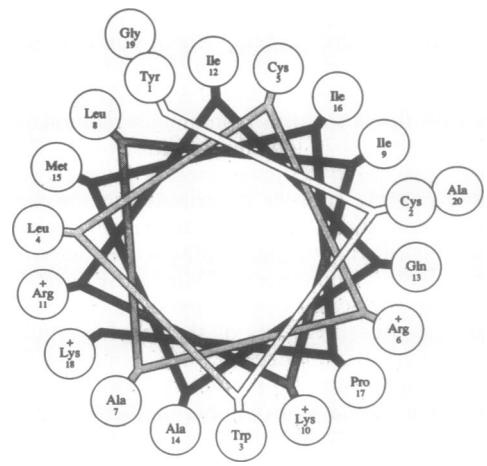


FIG. 1. Edmundson helical wheel diagram of residues Tyr-7 (position 1) to Ala-26 (position 20). Lysines and arginines occupy positions 6, 11, 10, and 18.

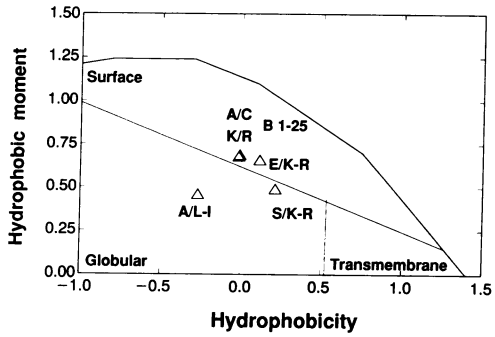


FIG. 2. Eisenberg plot of B(1–25) analogs. *x* axis, mean hydrophobicity per residue; *y* axis, mean hydrophobic moment per residue, based on a consensus hydrophobicity scale (21). Peptides are in one-letter code (Table 1).

**Surface Tension Measurements of Peptide/Lipid Interaction.** Adsorption and spreading of peptide/lipid dispersions, 2.4 mg/ml, were similarly studied in a King–Clements device. Estimates of adsorption were assessed by injecting 0.5-ml samples of peptide/lipid mixtures in 30 ml of saline (37°C, pH 5.3). Surface spreading was evaluated by loading 10-μl samples on the surface. Changes in surface tension were recorded for 120 sec, during which time >95% of the change in surface tension takes place.

Measurements of change in surface tension of peptide/lipid mixtures during compression were carried out at 37°C on unbuffered saline, in a modified Langmuir–Wilhelmy surface balance (KimRay, Greenfield Surfactometer, Oklahoma City, OK). Ten-microliter samples were loaded on a 51.5-$cm^2$ rectangular Teflon trough. Five 90-sec compression cycles of the surface film by 85% of the total area were carried out. Data were collected from the fifth run. Maximum and minimum surface tensions and the fraction of the total area at which surface tension fell below 10 mN/m (% area ≤ 10 mN/m), corresponding to the length of the collapse plateau, were used for comparison of the various dispersions.

## RESULTS AND DISCUSSION

Chou–Fasman analysis of the first 25 residues of the human SP-B sequence suggested a high probability of α-helical conformation for residues 10–22. Residues 15–25 had a high α moment and fell in the surface sector of the hydrophobic moment plot (21). Further examination of the amino-terminal domain using a Schiffer–Edmundson analysis (Fig. 1) showed segregation of polar residues from nonpolar ones in two distinct hemifaces, typifying amphipathic sequences (37).

Site-specific amino acid substitutions altered positioning of two synthetic peptides on the hydrophobic moment plot (Fig. 2). In the A/L-I sequence, the hydrophobicity and the hydrophobic moment decreased, thus moving this peptide to the globular region. S/K-R had a lower hydrophobic moment and an increased hydrophobicity, with plot coordinates within the globular sector. A/C, K/R, and E/K-R maintained plot coordinates similar to those of B(1–25).

Table 2. Apparent partition coefficients ($K_{ap}$) for B(1–25) analogs in surfactant lipid dispersions

| Peptide | $K_{ap}$, $(cm^{-3} \cdot mol^{-1}) \times 10^4$ |
|---|---|
| B(1–25) | 1.06 ± 1.42 |
| A/C | 0.64 ± 1.63 |
| A/L-I | 0.01 ± 0.06 |
| K/R | 1.43 ± 0.61 |
| S/K-R | 2.37 ± 1.42 |
| E/K-R | 1.75 ± 0.41 |

Peptide concentration in lipids, $[P]_L$, was estimated by subtracting the peptide concentration in the aqueous phase, $[P]_A$, from the total, $[P]_T$. The assumed lipid concentration = 1 g/ml. The apparent partition coefficient, $K_{ap}$, is from the equation $[P]_L = K_{ap} \times [P]_A$. $K_{ap}$ values are given as mean ± SD.

Table 3. Percent helical content based on analysis of CD spectra using unrestrained least-squares-fit algorithm and polylysine reference data

| | % helical content | | | |
|---|---|---|---|---|
| Peptide | 25% TFE | 50% TFE | 20 mM SDS | Lipid |
| B(1–25) | 50 | 75 | 75 | 75 |
| A/C | 50 | 80 | 80 | 80 |
| A/L-I | 20 | 55 | 70 | 20 |
| K/R | 60 | 75 | 75 | 75 |
| S/K-R | 55 | 75 | 70 | 65 |
| E/K-R | 25 | 60 | 70 | 20 |

TFE, trifluoroethanol/phosphate buffer (pH 5.3); SDS, SDS/PBS (pH 5.3); Lipid, DPPC:PG:PA, 68:22:9 (wt/wt) in saline (pH 5.3).

Measurements of peptide partitioning between lipid dispersion and bulk solvent are listed in Table 2. With the exception of the relatively hydrophilic A/L-I sequence, the other peptides, including B(1–25), were highly lipophilic.

CD spectroscopy was used to determine the overall helical content of synthetic B(1–25) analogs in several environments (Table 3). TFE/PBS solutions were used to test the tendency to express α-helical structures and to assess the sensitivity of this structure to changes in solvent polarity, in a helix-promoting solvent system (38). At 25% TFE/PBS, all peptides showed low helical content. Sequences with more hydrophilic residues (A/L-I) or a charge reversal (E/K-R) showed the lowest degree of α-helical structure in this relatively polar solvent system. Increasing TFE to 50% enhanced the helix content of B(1–25) and of the analogs. The CD spectra in TFE/PBS (1:1) were the same at pH 4.0, 5.3, and 7.0, suggesting that, within this pH range, the peptide conformation is stable. In this solvent system all peptides had a dominant α-helical structure, indicating that these sequences assume an α-helical configuration in specific environments.

To evaluate peptide conformations at a membrane-mimicking interface, CD spectroscopy was carried out using SDS micelles (30). All of the peptides adopted a dominant

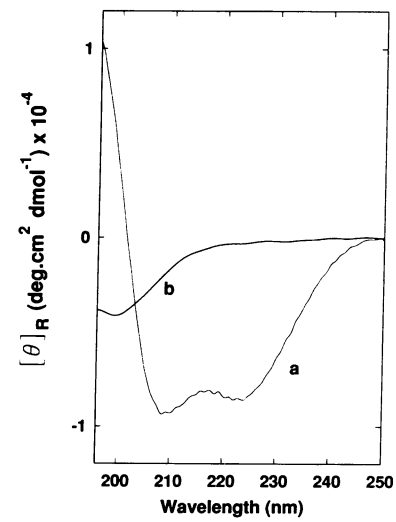


FIG. 3. CD spectra of synthetic peptides B(1–25) (curve a) and A/L-I (curve b) in Tanaka lipids [DPPC:PG:PA, 68:22:9 (wt/wt)], 154 mM NaCl/5 mM phosphate buffer, pH 5.3, 37°C. Curve a: double minima at 208 and 222 nm, marker of α-helical structure; curve b: disordered conformation (27, 28).

Table 4. Insertion parameters of synthetic B(1–25) in lipid monolayers and B(1–25) analogs in Tanaka lipid monolayers (DPPC:PG:PA)

| Lipid | Insertion parameter A | B | $\pi_c$ | Peptide | Insertion parameter A | $B/B_{exp}$ | $\pi_c$ |
|---|---|---|---|---|---|---|---|
| DPPC | −0.66 | 26 | 39 | B(1–25) | −0.66 | 30/24 ± 1 | 45 |
| DPPC:PG | −0.54 | 26 | 48 | A/C | −0.72 | 30/24 ± 1 | 42 |
| DPPC:PG:PA | −0.66 | 30 | 45 | A/L-I | −0.26 | 15/7 ± 1 | 57 |
| DPPC:SA:PA | −0.68 | 25 | 36 | K/R | −0.70 | 29/26 ± 0.1 | 42 |
| | | | | S/K-R | −0.54 | 18/19 ± 2 | 34 |
| | | | | E/K-R | −0.69 | 21/22 ± 2 | 31 |

A = slope of the plot of $\pi_i$ vs. $\Delta\pi$; B = theoretical equilibrium $\pi$ at $\pi_i = 0$; $B_{exp}$ = experimental equilibrium $\pi$ at $\pi_i = 0$; $\pi_c$ = critical pressure of insertion, in mN/m, at $\Delta\pi = 0$. Hypophase: 154 mM NaCl, 37°C, pH 5.3. Peptide concentration = 2.5 μM. Linear regression coefficients ($r$) for synthetic B(1–25) in lipid monolayers: 0.7–0.8, 8–18 data points per set. Linear regression coefficients ($r$) for B(1–25) analogs in Tanaka lipid monolayers: 0.8–0.9, 7–17 data points per set.

α-helical component. These results suggest that B(1–25) and the analogs preferentially assume helical conformations in an anionic micellar environment.

CD measurements of synthetic SP-B peptides in Tanaka lipid dispersions showed environment-dependent secondary structure. CD spectra for B(1–25) and A/L-I are shown in Fig. 3. B(1–25), A/C, and K/R all had high helical contents, as observed in 50% TFE/PBS and SDS micelles. S/K-R had a slightly lower helical content than B(1–25), and E/K-R and A/L-I had significantly lower helical content in lipid dispersions. After sedimentation of A/L-I by ultracentrifuge (60 min, 100,000 × $g$) the supernatant had the same CD spectra as the peptide/lipid dispersions, characterized by a largely disordered conformation. These findings confirmed that A/L-I preferentially associates with more polar environments, rather than with lipids. On the other hand, E/K-R associated with the lipids but had a decreased helical content, suggesting that peptide folding in anionic lipid was also dependent on peptide charge. Therefore, the α-helical content of the amphipathic segment in lipids appears to be dependent on charge and hydrophobicity of residues.

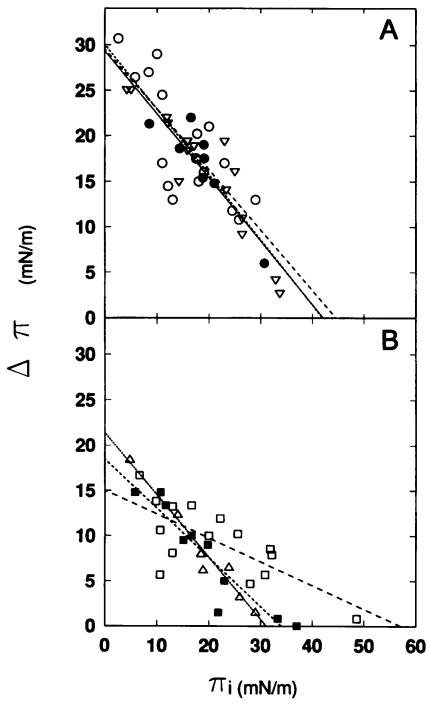


FIG. 4. Change in surface pressure ($\Delta\pi$) vs. initial surface pressure $\pi_i$ of a DPPC:PG:PA lipid monolayer. Hypophase as in Table 4. Peptide concentration, 2.5 μM. $x$ Axis, $\pi_i$ of the lipid monolayer; $y$ axis, $\Delta\pi$. ($A$) ○, B(1–25) ($n$ = 17); ●, A/C ($n$ = 8); ▽, K/R ($n$ = 15). ($B$) □ A/L-I ($n$ = 15); ■ S/K-R ($n$ = 10); △, E/K-R ($n$ = 7).

Since peptide/lipid interactions may alter light scattering of lipid vesicles, thereby affecting CD measurements, we used FTIR spectroscopy to complement the CD studies. FTIR measurements of B(1–25) analogs in Tanaka lipids showed bands between 1660 and 1650 $cm^{-1}$, typical of disordered and α-helical conformations (39, 42). There was no dominant band near 1630 $cm^{-1}$ indicative of β-sheet structures. These qualitative measurements suggest that the B(1–25) analogs assume largely disordered and α-helical structures in Tanaka lipid dispersions.

Critical pressure of insertion indicates partitioning of peptides between aqueous hypophase and lipid monolayer. Several lipid mixtures were compared to characterize the specificity of interaction of synthetic B(1–25) analogs with lipids. Results are shown in Table 4 (left side). B(1–25) had an intermediate $\pi_c$ in DPPC, a zwitterionic lipid. Addition of the anionic phospholipid PG to DPPC increased the $\pi_c$, indicating a higher affinity of the peptide for a negatively charged lipid monolayer. Addition of palmitic acid to the zwitterionic/anionic phospholipid mixture produced little change in $\pi_c$, suggesting that the fatty acid had little effect on binding and insertion of B(1–25). Replacement of PG by the positively charged lipid stearylamine in equimolar amounts decreased $\pi_c$, suggesting decreased interaction of the peptide with the monolayer. These results emphasize the role of anionic lipids in the interaction with B(1–25).

In subsequent experiments we used a monolayer of Tanaka lipids. Albumin, used as a standard at 1 μM, had a significantly lower $\pi_c$ than B(1–25) (40, 41). Results are shown in Table 4 (right side) at 2.5 μM. B(1–25) showed a $\pi_c$ of 45 mN/m. Peptides A/C and K/R had similar values of $\pi_c$. A/L-I had a high $\pi_c$ but presented an attenuated slope (A = 0.26), suggesting a relatively weak affinity for the interface,

Table 5. Surface tension values for adsorption and spreading of peptide/lipid dispersions

| Peptide | Adsorption 10 sec | Adsorption 120 sec | Spreading 10 sec | Spreading 120 sec |
|---|---|---|---|---|
| B(1–25) | 66 ± 4 | 55 ± 8 | 62 ± 3 | 56 ± 5 |
| A/C | 67 ± 4 | 54 ± 4 | 63 ± 5 | 57 ± 3 |
| A/L-I | 59 ± 3 | 51 ± 3 | 60 ± 1 | 57 ± 1 |
| K/R | 67 ± 4 | 57 ± 4 | 61 ± 7 | 57 ± 8 |
| S/K-R | 68 ± 3 | 58 ± 4 | 66 ± 3 | 62 ± 4 |
| E/K-R | 69 ± 2 | 62 ± 7 | 69 ± 2 | 67 ± 3 |
| Lipids | 69 ± 2 | 68 ± 2 | 68 ± 3 | 67 ± 3 |

Surface tension values are at 10 and 120 sec. Hypophase as in Table 4. Surface area, 44.2 $cm^2$. Adsorption: lipid concentration, 40 μg/ml; mean ± SD, 5–13 determinations. Spreading: lipid load, 24 μg; mean ± SD, 5–16 determinations.

Table 6. Surface tension of B(1–25) analogs in Tanaka lipids on a Langmuir–Wilhelmy surface balance

| Peptide | Max | Min | % <10 |
|---|---|---|---|
| B(1–25) | 58 ± 5 | 3 ± 2 | 49 ± 9 |
| A/C | 60 ± 4 | 0 ± 1 | 50 ± 6 |
| A/L-I | 60 ± 4 | 5 ± 1 | 53 ± 5 |
| K/R | 58 ± 4 | 5 ± 4 | 41 ± 6 |
| S/K-R | 62 ± 4 | 4 ± 4 | 33 ± 16 |
| E/K-R | 65 ± 2 | 6 ± 2 | 31 ± 4 |
| Lipids | 70 ± 2 | 55 ± 3 | — |

Max/Min = maximum/minimum surface tension, mN/m. % <10 = % of surface area with surface tension ≤10 mN/m. Hypophase as in Table 4. Surface area, 51.5 $cm^2$. Compression cycle: 90 sec, 85%. Lipid load, 24 μg; mean ± SD, 9–21 determinations.

as predicted by the hydrophobic moment plot. Coefficients A, slopes of the distributions, are otherwise similar for the remaining analogs (Fig. 4). S/K-R and E/K-R had a lower $\pi_c$ than B(1–25). E/K-R had a slightly higher $\pi_c$, when tested against a monolayer of DPPC:SA:PA, presumably because SA introduces positive charges in the monolayer. These observations support the hypothesis that electrostatic interactions between lipid head groups and peptide residues influence the insertion of an amphipathic helix in a lipid structure.

Dispersions containing S/K-R and E/K-R showed significantly different rates of adsorption and spreading, compared to B(1–25) ($P < 0.05$, by $t$ test) (Table 5), indicating that peptides that interact poorly with anionic lipids are less effective in enhancing adsorption and spreading of peptide/lipid dispersions.

Under compression, S/K-R and E/K-R had a significantly shorter collapse plateau than other dispersions ($P < 0.05$, by $t$ test), as shown in Table 6. These results are consistent with those obtained by measures of spreading, adsorption, and insertion. The collapse plateau for S/K-R manifested a wide variability (standard deviation of 50%), suggesting that this peptide/lipid dispersion constitutes nonhomogeneous populations of vesicles with different degrees of peptide/lipid affiliation.

We anticipated that the A/L-I peptide, with decreased hydrophobic moment, α-helical conformation, and affinity for lipids, would have decreased surface activity in peptide/lipid mixtures. Contrary to this expectation, adsorption rates and degree of surface compression to achieve low surface tension were similar to those found with B(1–25). We hypothesize that A/L-I affiliates with a lipid monolayer predominantly by means of electrostatic interactions, whereas other peptides bind to surface lipids by hydrophobic and electrostatic interactions. Peptide/lipid charge associations may therefore have more importance for peptide/lipid interaction and surface activity than degree of hydrophobicity, amphipathicity, or conformation.

In summary, the present investigation illustrates the role of individual residues in the interaction of B(1–25) with surfactant lipids. Behavior of B(1–25) in lipid dispersions mainly depends on electrostatic interactions and on hydrophobicity. Shape of residues and capacity for oligomerization by means of sulfhydryl links are less important. Inter- and intramolecular disulfide bond formation in the intact SP-B protein may also impose specific conformational constraints on other protein domains and have important effects on function. Study of full-length SP-B in oxidized and reduced forms is required to further define the role of oligomeric SP-B, the form of native SP-B, in surfactant lipids.

We thank Drs. Jan Dohlman for the helical wheel graphics, Jan Young and Richard Stevens for peptide synthesis, James McKnight and Lila Gierasch for their advice with CD analysis, and Frans J. Walther and Larry Gordon for review of the manuscript. This work was supported by National Institutes of Health Grant HL-40666 and by Research Centers in Minority Institutions Award RRO 3026 of the National Center for Research Resources of the National Institutes of Health.

1. Possmayer, F. (1988) *Am. Rev. Respir. Dis.* **138,** 990–998.
2. Pilot-Matias, T. J., Kister, S. E., Fox, J. L., Kropp, K., Glasser, S. W. & Whitsett, J. A. (1989) *DNA* **8,** 75–86.
3. Phelps, D. S. & Floros, J. (1988) *Am. Rev. Respir. Dis.* **137,** 939–942.
4. Weaver, T. E., Sarin, V. K., Sawtell, N., Hull, W. M. & Whitsett, J. A. (1988) *J. Appl. Physiol.* **65,** 982–987.
5. Hawgood, S. (1989) *Am. J. Physiol.* **257,** 13–22.
6. Hawgood, S. & Clements, J. A. (1990) *J. Clin. Invest.* **86,** 1–6.
7. Jacobs, K. A., Phelps, D. S., Steinbrink, R., Fisch, J., Kritz, R., Mitsock, L., Dougherty, J. P., Taeusch, H. W. & Floros, J. (1987) *J. Biol. Chem.* **262,** 9808–9811.
8. Curstedt, T., Johansson, J., Persson, P., Eklund, A., Robertson, B., Lowenadler, B. & Jornvall, H. (1990) *Proc. Natl. Acad. Sci. USA* **87,** 2985–2989.
9. Waring, A. J., Fan, B., Nguyen, T., Amirkhanian, J. D. & Taeusch, H. W. (1990) *Prog. Respir. Res.* **25,** 343–346.
10. Fan, B. R., Nguyen, T., Waring, A. & Taeusch, H. W. (1990) *Anal. Biochem.* **186,** 41–45.
11. Takahashi, A. & Fujiwara, T. (1986) *Biochem. Biophys. Res. Commun.* **135,** 527–532.
12. Notter, R. H., Shapiro, D. L., Ohning, B. & Whitsett, J. A. (1987) *Chem. Phys. Lipids* **44,** 1–17.
13. Hawgood, S., Benson, B. J., Schilling, J., Damm, D., Clements, J. A. & White, R. T. (1987) *Proc. Natl. Acad. Sci. USA* **84,** 66–70.
14. Mathialagan, N. & Possmayer, F. (1990) *Biochim. Biophys. Acta* **1045,** 121–127.
15. Suzuki, Y., Fujita, Y. & Kogishi, K. (1989) *Am. Rev. Respir. Dis.* **140,** 75–81.
16. Sarin, V. K., Gupta, S., Leung, T. K., Taylor, V. E., Ohning, B. L., Whitsett, J. A. & Fox, J. L. (1990) *Proc. Natl. Acad. Sci. USA* **87,** 2633–2637.
17. Waring, A. J., Taeusch, H. W., Bruni, R., Amirkhanian, J. D., Fan, B., Stevens, R. & Young, J. (1989) *Pept. Res.* **2,** 308–313.
18. Baatz, J. E., Elledge, B. & Whitsett, J. A. (1990) *Biochemistry* **29,** 6714–6720.
19. Shiffer, K., Hawgood, S., Duzgunes, N. & Goerke, J. (1988) *Biochemistry* **27,** 2689–2695.
20. Eisenberg, D., Weiss, R. M., Terwilliger, T. C. & Wilcox, W. (1982) *Faraday Symp. Chem. Soc.* **17,** 109–120.
21. Takahashi, A., Waring, A. J., Amirkhanian, J., Fan, B. & Taeusch, H. W. (1990) *Biochim. Biophys. Acta* **1044,** 43–49.
22. O'Neil, K. T. & DeGrado, W. F. (1990) *Science* **250,** 646–651.
23. Chou, P. Y. & Fasman, G. D. (1978) *Adv. Enzymol.* **47,** 45–148.
24. Schiffer, M. & Edmundson, A. (1967) *Biophys. J.* **7,** 121–135.
25. Stewart, J. M. & Young, J. D. (1984) in *Solid Phase Peptide Synthesis* (Pierce Chemical, Rockford, IL).
26. Tanaka, T., Takei, T., Aiba, K., Masuda, K., Kiuchi, A. & Fujiwara, F. J. (1986) *Lipid Res.* **27,** 475–485.
27. Johnson, W. C., Jr. (1990) *Proteins* **7,** 205–214.
28. McKnight, C. J., Briggs, M. S. & Gierasch, L. M. (1989) *J. Biol. Chem.* **264,** 17293–17297.
29. Greenfield, N. & Fasman, G. D. (1969) *Biochemistry* **8,** 4108–4115.
30. Rafalski, M., Lear, J. D. & DeGrado, W. F. (1990) *Biochemistry* **29,** 7917–7922.
31. Gierasch, L. M. (1989) *Biochemistry* **28,** 923–930.
32. Batenburg, A. M., Demel, R. A., Verkleij, A. J. & de Kruijff, B. (1988) *Biochemistry* **27,** 5678–5685.
33. Segrest, J. P., Jackson, R. L. & Gotto, A. M. (1974) *FEBS Lett.* **38,** 247–253.
34. Mayer, L. D., Nelsestuen, G. L. & Brockman, H. L. (1983) *Biochemistry* **22,** 316–321.
35. Verger, R. & Pattus, F. (1982) *Chem. Phys. Lipids* **30,** 189–227.
36. Phillips, M. C. & Sparks, C. E. (1980) *Ann. N.Y. Acad. Sci.* **348,** 122–137.
37. Segrest, J. P., De Loof, H., Dohlman, J. G., Brouillette, C. G. & Anantharamaiah, G. M. (1990) *Proteins* **8,** 103–107.
38. Zahler, P. & Niggli, V. (1977) *Methods Membr. Biol.* **8,** 1–22.
39. Surewicz, W. K. & Mantsch, H. H. (1988) *Biochim. Biophys. Acta* **952,** 115–130.
40. Carter, D. C., He, X., Munson, S. H., Twigg, P. D., Gernert, K. M., Broom, M. B. & Miller, T. Y. (1989) *Science* **244,** 1195–1198.
41. Holm, B. A., Enhorning, G. & Notter, R. H. (1988) *Chem. Phys. Lipids* **49,** 49–55.
42. Cornell, D. G., Dluhy, R. A., Briggs, M. S., McKnight, J. & Gierasch, L. M. (1989) *Biochemistry* **28,** 2789–2797.